Thermal Nondestructive Evaluation Report Inspection of the Refurbished Manipulator Arm System in the Manipulator Development Facility at Johnson Space Center 10-12 January 2001

K. Elliott Cramer
NASA Langley Research Center
4 Langley Blvd. – MS231
Hampton, VA 23681
(757) 864-7945
k.e.cramer@larc.nasa.gov

Introduction

On 10-12 January 2001, inspections were performed on the face of the lower and upper arms of the Refurbished Manipulator Arm System (RMAS) in the Manipulator Development Facility (MDF) at Johnson Space Center (JSC). Figure 1 shows a block diagram of the inspection system used in the inspection. The thermal images are produced with a commercial infrared (IR) radiometer (Raytheon / Amber model Radiance 1n) which uses a Indium-Antominide (InSb) staring focal plane array detector cooled to near liquid nitrogen temperatures by an closed cycle electric microcooler. The radiometer's noise equivalent temperature difference (NEDT), cited by the manufacturer, is 0.025°C when operating the detector in the 3 to 5 micrometer wavelength range. The radiometer produces images at both 30 frames per second output (video frame rate, in an RS170, format compatible with standard video equipment) and 60 frames per second output in a 12-bit, RS422 digital format. External optics, consisting of a wide-angle lens, using germanium optical elements, was used to increase the system field-of-view by a factor of approximately two. This lens has a field-of-view of 22° in both the horizontal and vertical directions.

The heat source used consists of two commercially available quartz lamps (750 Watts each) which are mounted on either side of the IR camera. Quantitative time based analysis requires synchronization between the IR imager, the heat source. This synchronization is achieved by computer control of the application of heat and the data acquisition. For all cases presented in this paper the maximum surface temperature change of the sample above ambient never exceeded 10°C.

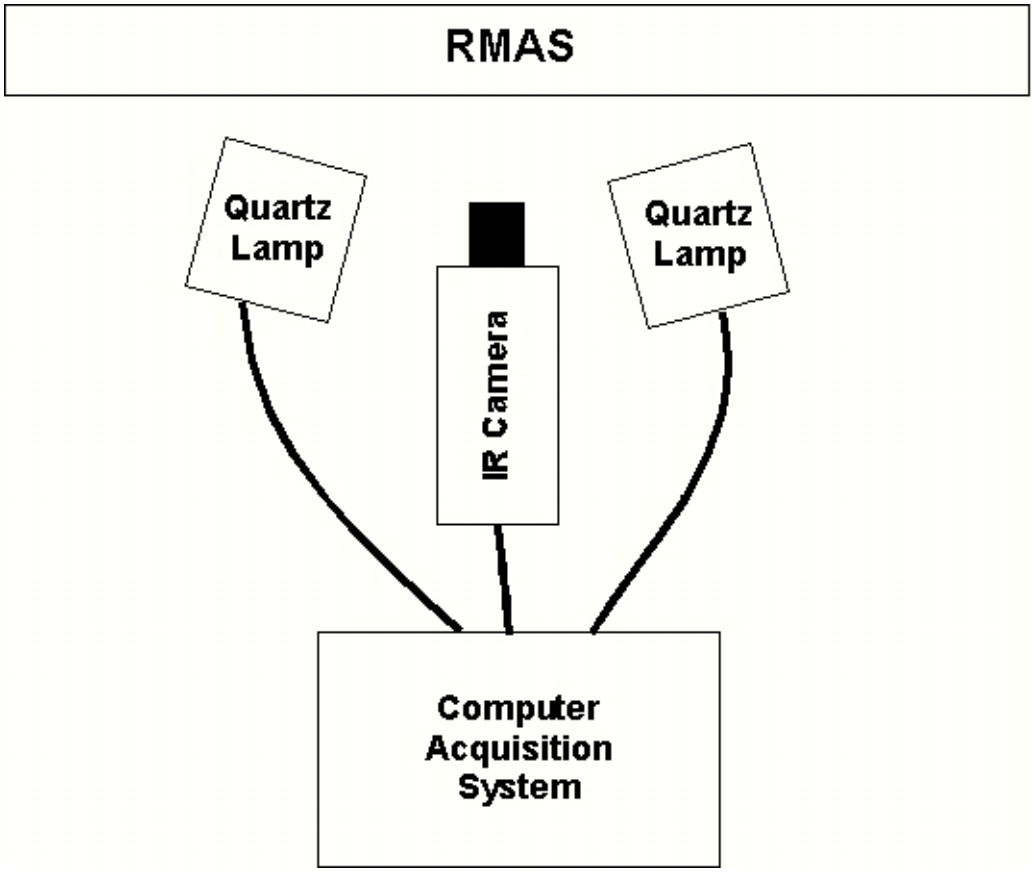

Figure 1 -- LaRC Thermal Imaging System

The digital data from the radiometer is acquired and stored at a maximum of 60 frames-per-second in a real-time image processor board in the control computer. The image processor board has 256 megabytes of image memory available for storage and is capable of real-time floating point processing of the incoming data. From a set of acquired images, a single image is then reconstructed that represents the instantaneous rate of change of the temperature immediate after the heat source is turned off. The image processor does the reconstruction after the data has been collected and stored to the control computer's hard disk. All of the data presented in the remainder of the paper (unless otherwise noted) were reconstructed in this manner.

Because the RMAS has low emissivity surfaces, it is necessary to enhance the emissivity by coating the surface. For the results presented here, the samples are treated with water washable, nontoxic paint (Krylon® Washable Tempera Paint), to enhance the emissivity.

Data Collection

To initially assess the viability of thermal imaging to inspect the RMAS Arm material and to establish the inspection parameters a cursory inspection of test coupon was performed. From this inspection a calculation of the thermal diffusivity was performed[1]. The thermal diffusivity was found to be 0.004 cm^2/s[*].

The results of the thermal diffusivity measurement were then used to establish the inspection parameters. Digital data from the IR radiometer was collected a 30 frames per second, and every 14 consecutive frames were averaged together to enhance signal to noise. Heat from the quartz lamps was applied for 40 seconds and data was collected for an additional 120 seconds after the heat was removed. After storage, the resulting time series of temperature images was reduced to a single image by calculating the instantaneous time derivative immediately after the removal of the heat source (the final image in the series was used to normalize the time derivative to remove the effects of uneven heating)[2]. Figure 2 show photographs of the IR camera and quartz heaters (both on and off) during an inspection of the upper arm.

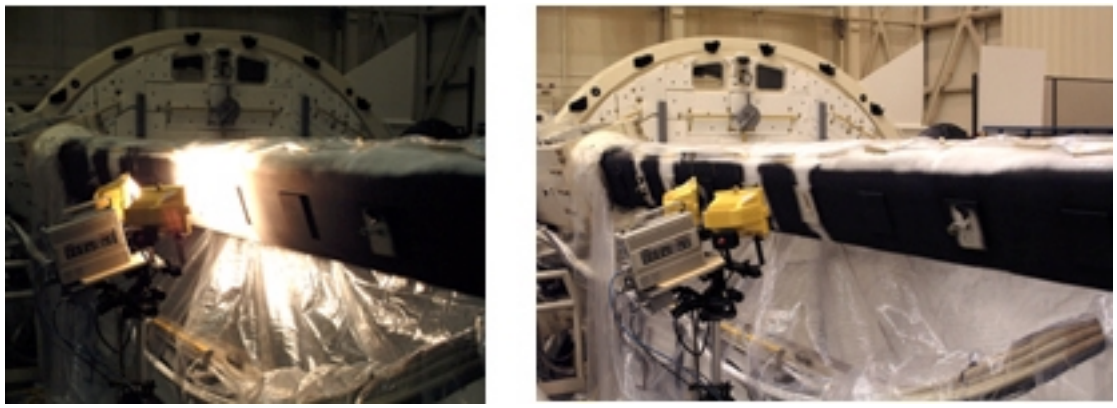

Figure 2 -- LaRC Thermal System During Inspection of RMAS

[*] The accuracy of this measurement is unknown for several reasons. First, the coupon inspected was from the end of one of the RMAS, which has a construction that differs from the central arm regions. Second, since only one coupon was available it is impossible to access the accuracy or repeatability of the thermal diffusivity measurements for this material system.

Inspection Areas

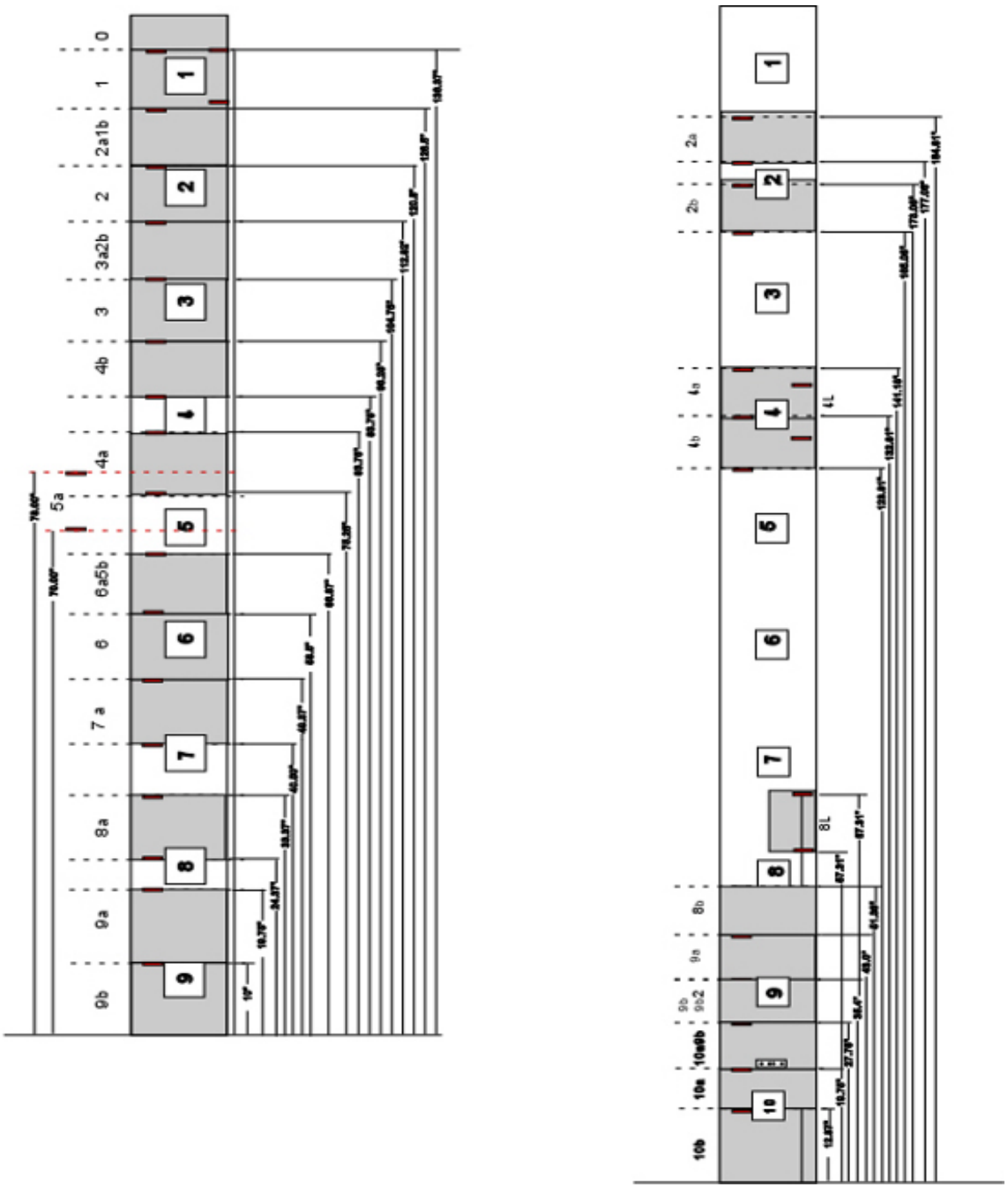

a b

Figure 3 -- Inspection Areas on the (a) Upper and (b) Lower Arm

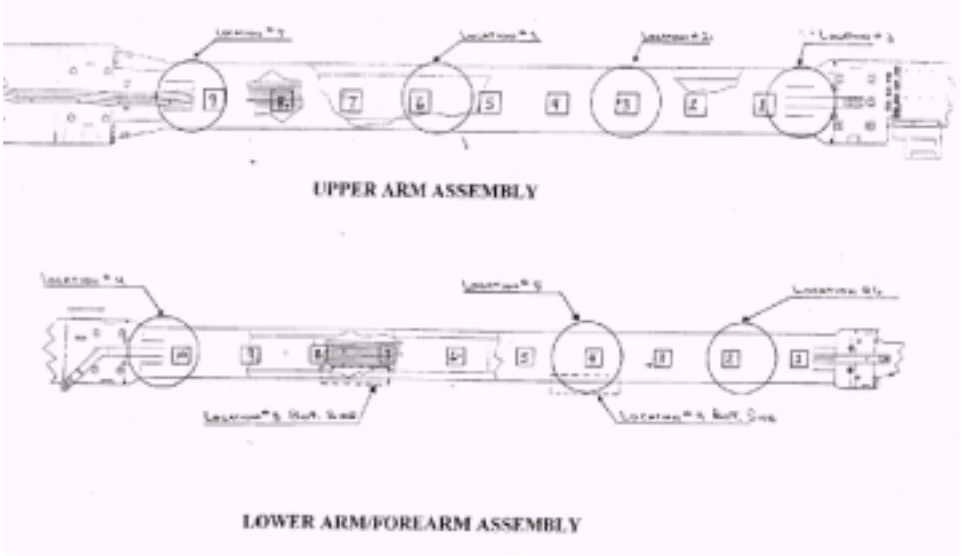

Figure 4 -- JSC Defined Locations of Interest for Inspection

Inspection Results Summary

Composite thermal images for Locations 1-9 are shown on pages 9-13 of this report. In many of the images where inspections were performed close to the mounting pads a darkening of the image occurs on either side of the pad. This darkening is the result of both the changes in heat flow in the composite and nonuniformities in the application of heat due to the presence of the pad. These areas are not as pronounced above and below the pads because of the orientation of the quartz heat lamps relative to the pads (see Figure 1).

The general mottling observable in the images is typical of thermal data and does not represent indications of defects or damage. This mottling is due primarily to stretching of the contrast of the image in an attempt to utilize the full range of gray level available in the computer. The determination of indications is accomplished by looking at the time-resolved data which is difficult to present in written form.

Location #1:

No indications of material degradation were recorded in the thermal inspection. Note that the fiber lay-up is clearly visible in this image.

Location #2:

Several small indications were recorded, especially between pad #2 and pad #3. These indications are consistent with a reduction in thermal

heat flow into the material, which could be due to a number of factors such as porosity, resin rich regions or localized delaminations[#].

The two indications above pad #3 are also consistent with a reduction in thermal heat flow, but are of a larger extent. The time resolved data reveals that these indications appear to be limited in extent to very close to the surface.

Indication Sizes:

#1 – 1.4 in. wide x 1.1 in. high

#2 – 0.9 in. wide x 0.8 in. high

#3 – 0.3 in. long

#4 – 0.4 in. long

#5 – 0.35 in. long

Location #3:

Directly below pad #1 the visible surface damage can also be seen in the IR images. This damage appears to be limited in extent to the near surface region and does not display thermal characteristics of impact damage that has resulted in subsurface delaminations.

Between pad #1 and the elbow indications were observed which are consistent with wrinkles in the composite material.

Additionally, just above the right corner of pad #1 is a small indication[#] consistent with those seen throughout both the upper and lower arms (see note on location #2).

Indication Sizes:

#1 – 0.9 in. wide x 0.6 in. high

#2 – 0.8 in. wide x 0.7 in. high

#3 – 0.32 in. long

Note: It was not possible to make measurements of the size of the wrinkles because of the large camera angle required to access this location.

[#] Note: These small indications are seen throughout the upper and lower arm, even in areas where no impact is suspected, which may indicate that they are a result of the manufacture of the structure.

Location #4:

One indication was recorded between pad #10 and the elbow. This indication (although larger) is consistent with the small indications[#] seen throughout both arms (see note on location #2).

Indication Sizes:

#1 – 1.35 in. wide x 0.3 in. high

Locations #5 & #9:

A number of significant indications were observed in these locations. First, a large vertical indication parallel and to the left of pad #4 was observed. This indication appears to extend quite deep into the material (at least through ½ the thickness) and also tends to spread parallel to the fibers. Again this is a region that does not allow good propagation of the heat flux and could be attributed to porosity, dry fibers (resin poor regions) or delaminations.

Another series of indications were recorded directly below pad #4. These indications do not appear to follow the fiber layup and also extend quite deep into the material.

Indication Sizes:

#1 – 0.8 in. wide x 0.5 in. high

#2 – 0.8 in. wide x 0.6 in. high

#3 – 0.5 in. wide x 0.8 in. high

#4 – 0.8 in. wide x 6.25 in. high

Location #6:

Four indications were recorded between pad #2 and pad #1. These indications are consistent with the small indications[#] seen throughout both arms (see note on location #2).

Indication Sizes:

#1 – 1.7 in. wide x 0.3 in. high

#2 – 0.8 in. wide x 0.3 in. high

#3 – 0.8 in. wide x 0.2 in. high

#4 – 0.4 in. wide x 0.3 in. high

Location #7:

Between pad #9 and the shoulder indications were observed which are consistent with wrinkles in the composite material as seen in Location #3.

Indication Sizes:

#1 – 2.8 in. long

#2 – 3.8 in. long

Location #8:

Between pads #7 & #8 a single indication was observed which is consistent with impact damage indications that have been observed in other composite materials. This indication is fairly localized on near the surface, but appears to grow in size deeper into the material.

Indication Sizes:

#1 – 2.2 in. wide x 0.6 in. high

Conclusions

While numerous indications were recorded in both the suspect locations and in other areas, it is extremely difficult to accurately interpret the results with out either a baseline inspection of the RMAS against which the current inspection can be compared. Appropriate standards to calibrate the inspection procedures and results are required.

Some indications are observed that could potentially indicate damage that resulted from the impact the RMAS sustained, but no absolute conclusions can be drawn given the inspection circumstances.

Certain areas (Locations 5, 8 and 9) showed indications unique enough to warrant further investigation of these with other techniques such as conventional and advanced ultrasound or x-ray.

Inspection Results by Location of Interest

The collage of images that follow are representative of the results obtained using the LaRC Thermal NDE technique. These images are only a subset of all the data obtained.

Upper Arm

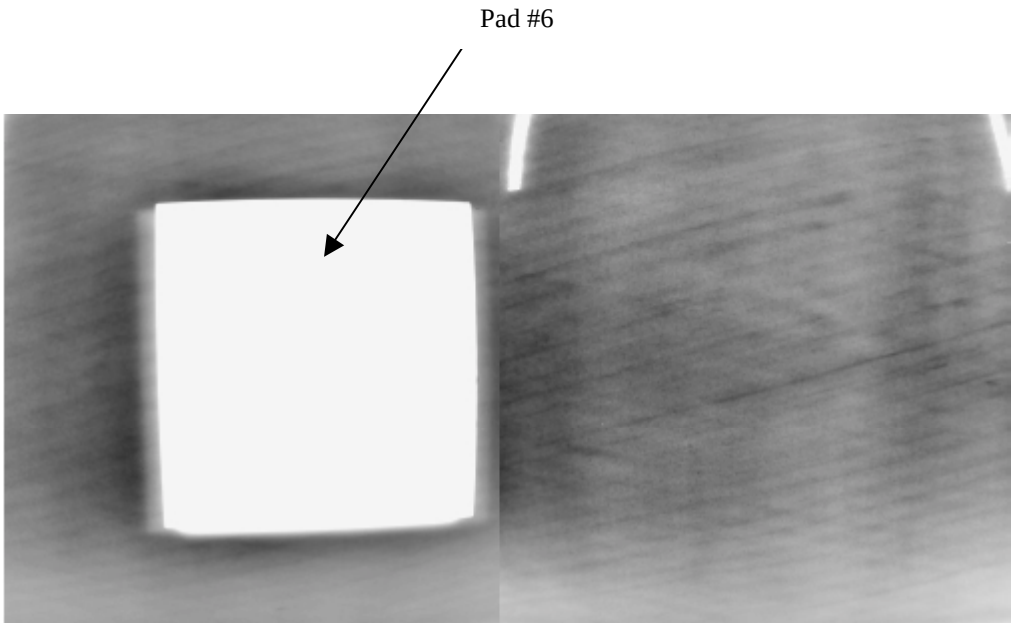

Location #1
No Indications Recorded

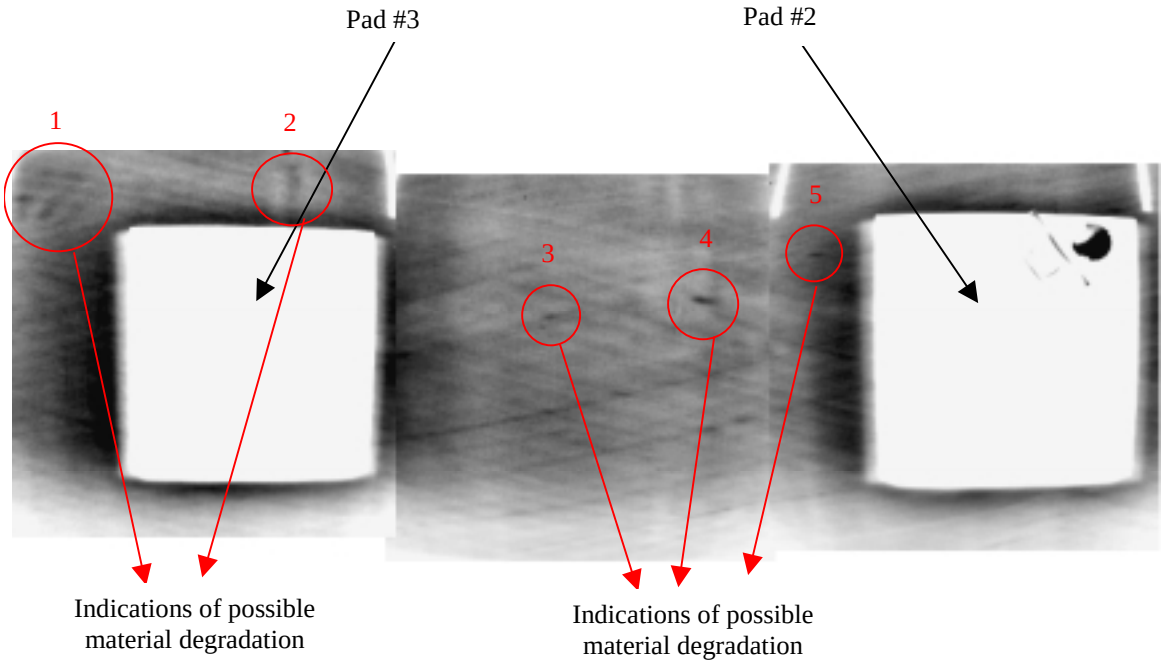

Location #2

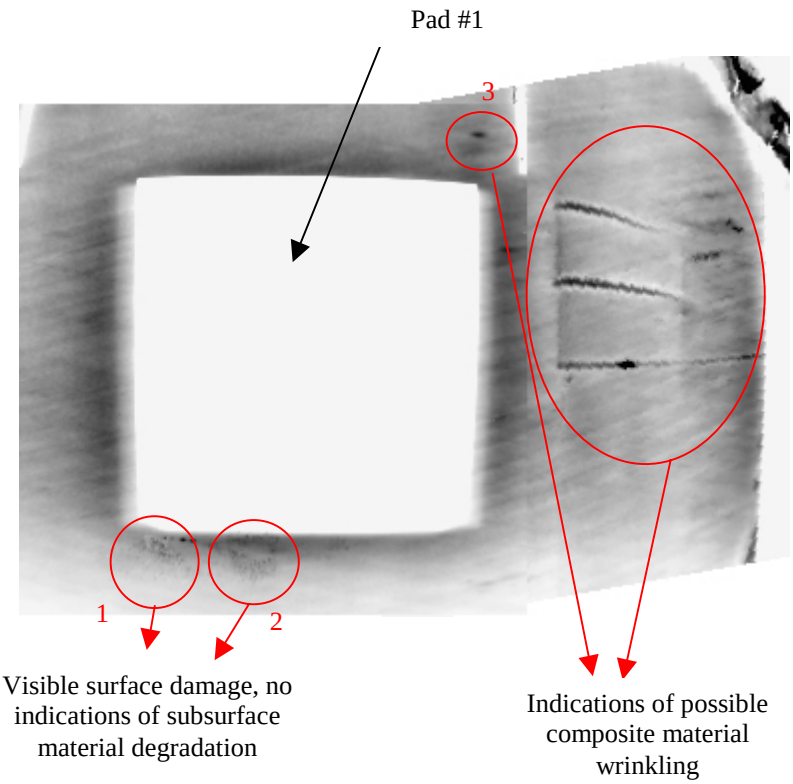

Location #3

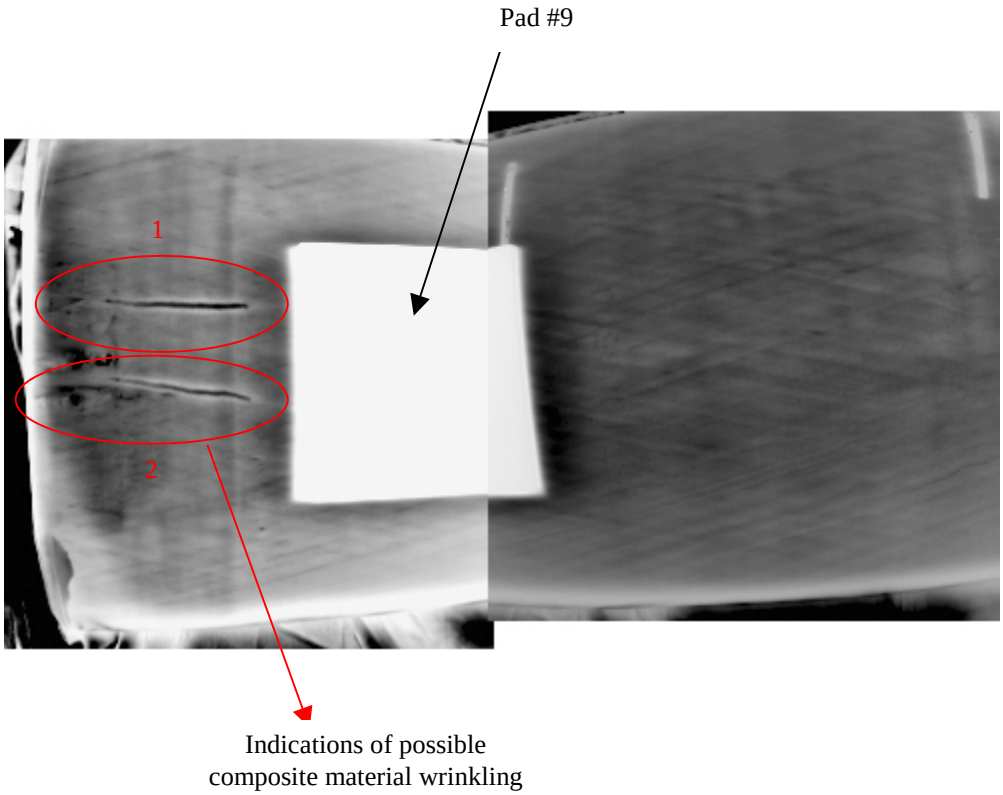

Location #7

Lower Arm

Pad #10

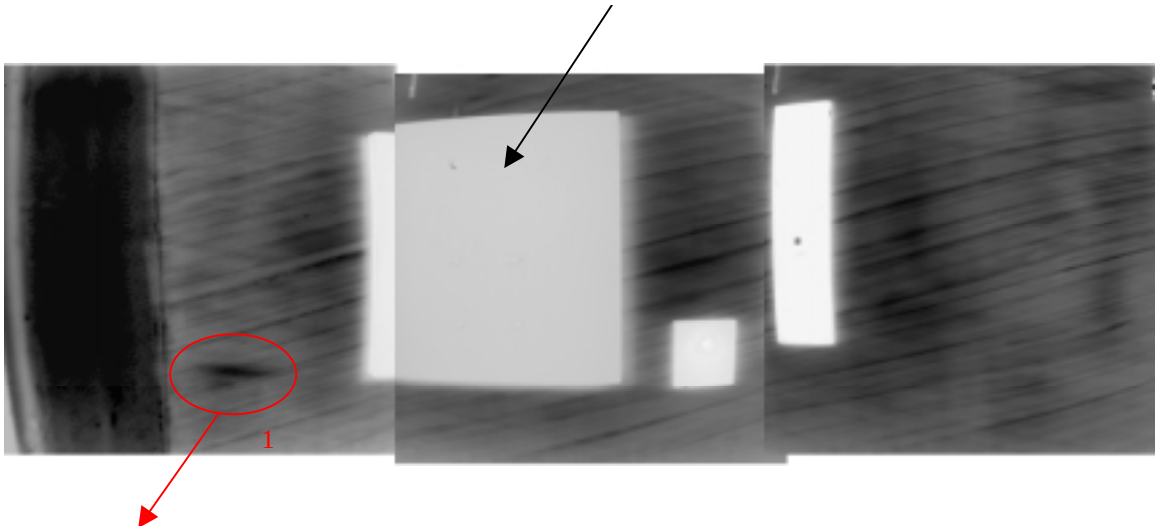

Indication of potential material degradation

Location #4

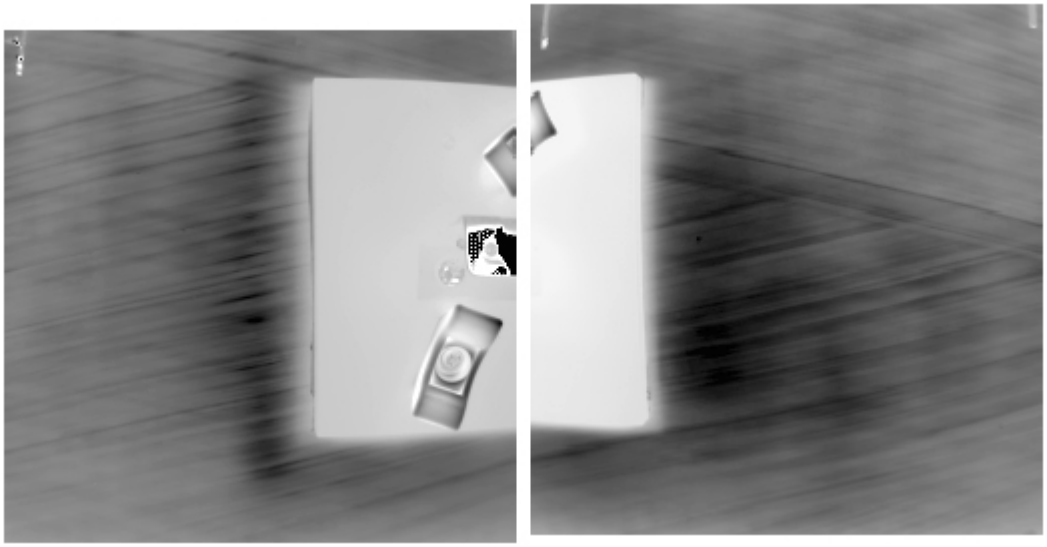

Pad #9
No Indications (Recorded for Reference)

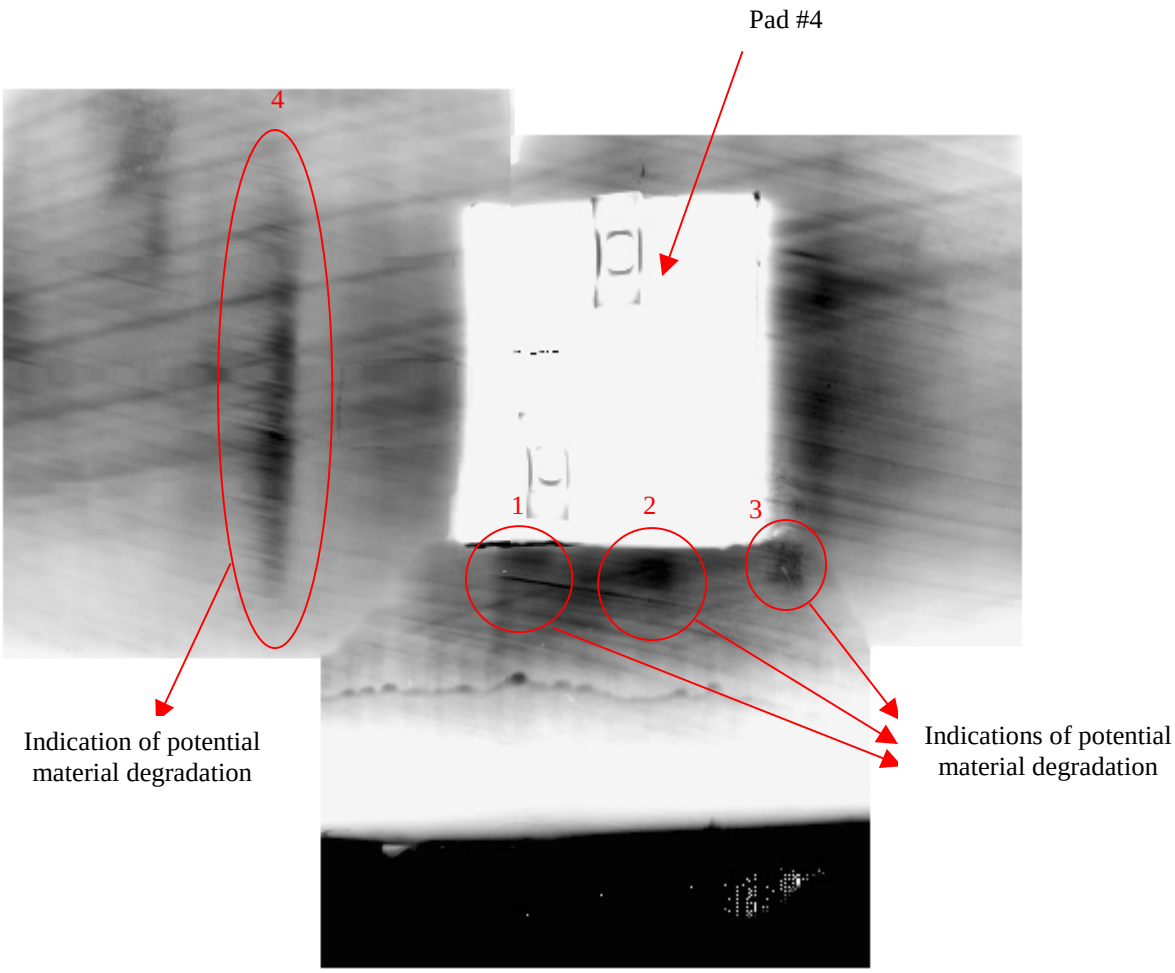

Locations #5 & #9

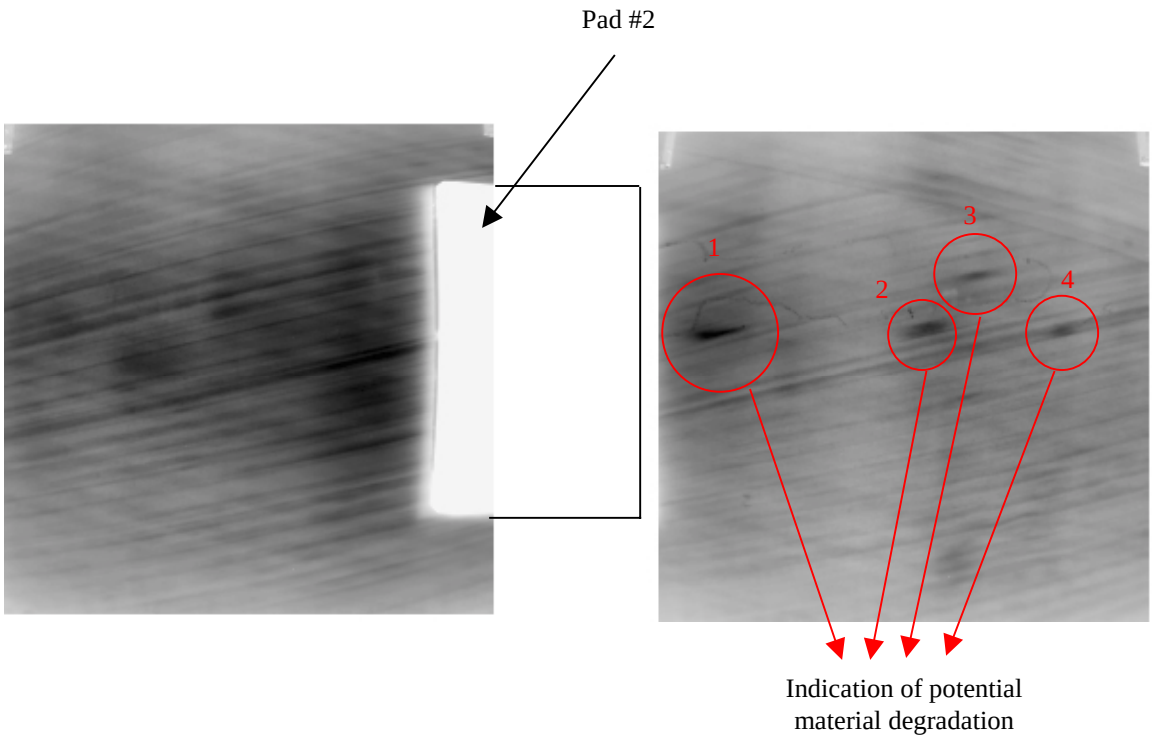

Location #6

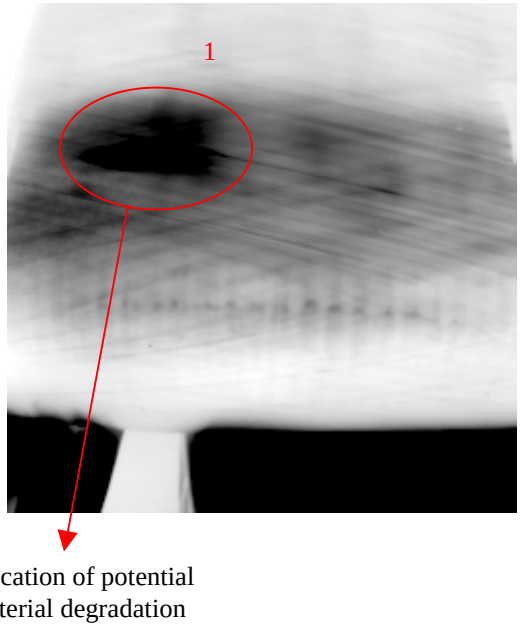

Location #8

References

1. K.E. Cramer, W.P.Winfree, E.R. Generazio, R. Bhatt and D.S. Fox, *Review of Progress in Quantitative Nondestructive Evaluation*, Vol. 12, ed. D.O. Thompson and D.E. Chimenti (Plenum Press, New York, 1993), p. 1305.
2. K.E. Cramer, P.A. Howell and H.I. Syed, *Proceedings SPIE - Thermosense XVII,*Vol. 2473, ed. S. A. Semanovich (SPIE,Bellingham,1995), p. 226.